Maximizing Plant Potential: Harnessing Microgrid Controllers for Peak Shaving and Energy Arbitrage in South Africa's Evolving Independent Power Producer Market

Cuan Bainbridge and Jaco Jansen Van Rensburg
Setcon

Manas Chakraborty, Nabeel Nisam, and Muthuraman Shanmugam
Schweitzer Engineering Laboratories, Inc.

Presented at the
22nd Annual CIGRE GCC International Conference
Muscat, Oman
November 2-4, 2026

Maximizing Plant Potential: Harnessing Microgrid Controllers for Peak Shaving and Energy Arbitrage in South Africa's Evolving Independent Power Producer Market

Cuan Bainbridge and Jaco Jansen Van Rensburg, *Setcon*
Manas Chakraborty, Nabeel Nisam, and Muthuraman Shanmugam, *Schweitzer Engineering Laboratories, Inc.*

***Abstract*—Microgrids have emerged as a vital solution for integrating distributed energy resources (DERs), enhancing the efficiency, reliability, and resilience of modern electrical systems. Their effective operation requires seamless coordination among DERs, loads, and energy management strategies to ensure optimal performance while adhering to technical and economic constraints. This paper reviews the implementation of a microgrid control system (MCS) comprising over 2.112 MVA of grid-tied photovoltaic (PV) inverter capacity across six inverters, a 4,586 kWh battery energy storage system (BESS), and a 1.6 MVA diesel generator for a shopping center in Tshwane, South Africa. The focus is on the high-level operation and coordination of these components.**

The project architecture integrated a new microgrid controller with existing assets to perform economic dispatch, peak shaving, and autosynchronization. A simulator was developed for system validation prior to commissioning, with simulation results compared against live operating data. Energy arbitrage is achieved by classifying weekday hours as peak, standard and off-peak modes. During peak periods, the BESS discharges to reduce grid demand, with generator support when PV output or battery state of charge is insufficient. During off-peak periods, the BESS charges while grid imports remain within peak-shaving limits. A voltage difference–based autosynchronization method for a BESS operating in virtual synchronous generator (VSG) mode is also explored. The inverter adjusts its output voltage and phase angle accordingly, while the VSG mode emulates inertia to maintain frequency stability. This paper outlines technologies and design strategies used to implement a robust and efficient MCS.

***Keywords*—Microgrid control system, battery energy storage system, photovoltaic, virtual synchronous generator, energy arbitrage, peak shaving, energy price, point of utility connection.**

I. Introduction

Microgrids are localized power systems capable of operating either in grid-connected or islanded mode. They typically integrate distributed energy resources (DERs) such as photovoltaic (PV) systems, wind turbines, and energy storage units. The effectiveness of a microgrid is determined by its ability to maintain stable and reliable operation under varying system conditions, including fluctuations in generation and load demand, as well as potential disconnection from the main utility grid.

A contemporary microgrid must coordinate multiple energy assets, including utility interconnections, a battery energy storage system (BESS), PV arrays, and diesel generators. This coordination requires seamless interoperability with distributed controllers. This complex coordination landscape is governed by the microgrid control system (MCS), which serves as the centralized intelligence layer, ensuring synchronized operation across all subsystems.

At the core of the MCS lies an economic dispatch algorithm that optimizes energy flow, storage utilization, and load management under dynamic constraints. This includes real-time coordination of assets to minimize grid import, particularly during peak tariff periods, and prioritize BESS charging during off-peak and nocturnal intervals to enhance cost efficiency. The system is designed to facilitate seamless transitions between grid-connected and islanded modes, leveraging a fast-response BESS and intelligent asset coordination to maintain power quality and continuity without disruption.

The proposed framework emphasizes advanced control logic to enable seamless and rapid mode transitions, while integrating economic objectives within the dispatch strategy. The design approach prioritizes optimal utilization of local energy resources and reduces reliance on the utility grid, thereby enhancing system resilience and achieving cost-effective operation.

II. Problem Statement and Research Gap

Microgrids integrating PV inverters, BESSs, and diesel generators provide a path toward more resilient, efficient, and sustainable power systems. However, the coordination of these DERs remains a challenge. Operators must balance real-time power flows, maintain stability during grid synchronization, and optimize economic performance through strategies such as energy arbitrage, peak shaving, and demand-side management. In South Africa's Tshwane region, frequent load-shedding events and infrastructure-related outages increase the need for autonomous and resilient microgrid operation. Microgrids must maintain supply to critical loads, optimize limited generation and storage resources, and transition seamlessly between grid-connected and islanded modes while preserving stability and cost-effectiveness. Existing microgrid solutions address aspects of these challenges, but significant gaps remain:

- Fragmented control: DERs are often managed independently, reducing overall efficiency.

- Weak synchronization robustness: Conventional methods can cause surges and frequency deviations during grid reconnection.
- Limited economic optimization: Arbitrage strategies often fail to adapt to changing tariffs, state-of-charge (SOC) levels, renewable generation, and load-shedding schedules.
- Insufficient validation: Testing is commonly limited to commissioning, increasing costs and the risk of operational errors.

These gaps are addressed through implementation and evaluation of an MCS tailored to South Africa's grid challenges. The system integrates multisource coordination and dispatching from the BESS, advanced synchronization using the voltage difference (ΔV) method in virtual synchronous generator (VSG) mode, and robust energy arbitrage strategies. A simulation environment strengthens the approach, allowing precommissioning validation and continuous improvement. By doing so, the work advances the state of microgrid control, providing a framework that enhances efficiency, stability, and economic performance across standalone and grid-connected applications while ensuring resilience despite frequent load-shedding events.

III. South Africa–Related Research and Data

Table I lists high and low demand tariffs for Tshwane. Demand is split into a high season (June–August) and a low season (the rest of the year).

TABLE I
HIGH AND LOW DEMAND TARIFFS (ZAR/USD) FOR TSHWANE

High Demand			Low Demand		
Hours	ZAR	USD	Hours	ZAR	USD
Peak	5.8113	0.3315	Peak	2.2261	0.1269
Standard	2.1226	0.1211	Standard	1.3751	0.0784
Off-Peak	1.1313	0.0645	Off-Peak	0.9731	0.0555

Fig. 1 assumes a standard load profile. Under this condition, 32.5% of low-demand energy is consumed in a 5-hour window (7–9 a.m. and 6–9 p.m.)—about 20.8% of the day—highlighting the temporal skew of energy charges even under uniform demand.

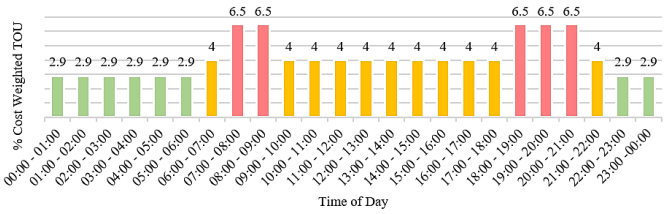


Fig. 1 Low-demand cost-weighted bar chart.

Fig. 2 shows the low-demand energy charge distribution under an assumed standard load profile; 47.5% of total energy charges occur within a 5-hour window, equivalent to 20.8% of a full day. When a realistic load profile is applied to this model, the hourly cost disparity observed in the standard load scenario may either be mitigated or intensified, depending on the consumption pattern.

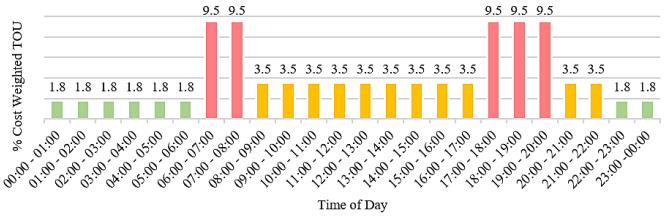


Fig. 2 High-demand cost-weighted bar chart.

The high-demand time-of-use (TOU) profile was applied to real load data from a Tshwane shopping center, comparing actual and modeled cost behavior, which reveals that PV integration has minimal impact on peak-period energy costs. The Tshwane tariff for maximum demand charge for an 11 kV supply scale is around 290.0996 ZAR/kVA, which is equivalent to 16.5487 USD/kVA, and it is a major contributor to electricity costs. Unlike energy charges, it is an availability charge based on the highest recorded client demand, measured at the point of utility connection (PUC). As shown in Fig. 3, PUC demand is recorded as half-hourly average kVA; the highest value sets the monthly maximum demand charge, reflecting the customer's peak demand on the utility network. Fig. 3 shows the highest value at 2,937.27 kVA for the month, the cost of which is shown in Table II.

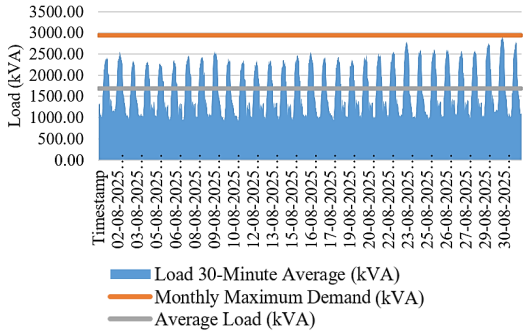


Fig. 3 Monthly maximum demand measurement.

TABLE II
USE-CASE MAXIMUM DEMAND CHARGE

Actual Maximum Demand	2,937.27 kVA
Cost ZAR	852,100.8654
Cost USD	48,608.1497

The maximum demand charge equals the demand rate (ZAR/kVA) multiplied by the measured maximum demand, so higher peak demand directly raises monthly costs. To illustrate peak shaving, the recorded maximum kVA was reduced to the average billing-period kVA. The resulting savings are shown in Table III—about ZAR 360,588.50 (USD 20,569.80) per month, underscoring the economic value of demand management and BESSs. The modified load profile in Fig. 4 shows the ideal outcome, with peak demand limited to the average load level. However, in actuality, the peak-period energy reduction must be shifted to off-peak periods to recover the deficit at a lower cost.

TABLE III
POST-PEAK-SHAVING MAXIMUM DEMAND COST

Standard Average Maximum Demand	1,694.29 kVA
Cost ZAR	491,512.3466
Cost USD	28,038.3541

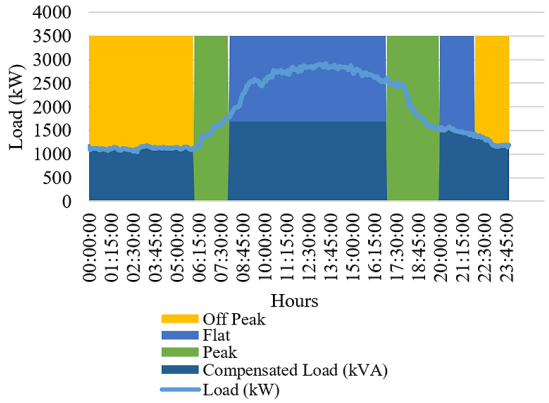


Fig. 4 Ideal compensated load as seen from PUC

Fig. 5 illustrates that the energy recovered in off-peak periods is insufficient to fully offset the energy deficit created by peak-reduction measures; load shifting alone cannot achieve complete demand balance. To address the shortfall, alternative energy sources, e.g., BESSs or onsite generation, should be employed along with off-peak energy use for a more stable, cost-efficient load profile. A global control system that monitors the entire facility, like a microgrid controller, achieves this.

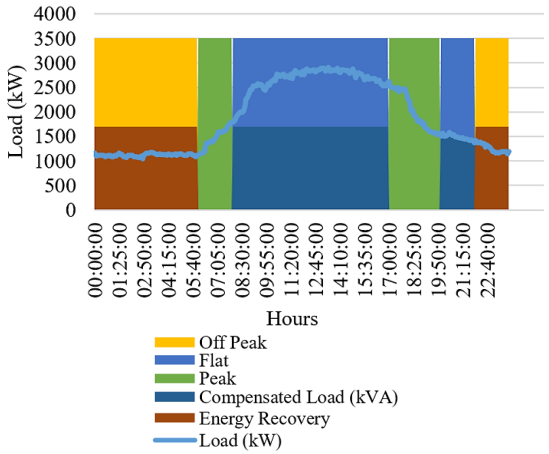


Fig. 5 Ideal compensated load with energy recovery as seen from PUC.

IV. MCS DESIGN OVERVIEW

This paper presents engineering and validation best practices for an MCS and outlines standard control and protection functions. The project architecture features a microgrid controller integrated with existing PV inverters, a BESS, and diesel generators. Three strategies were implemented to optimize energy consumption and plant performance: 1.) economic dispatch and peak shaving in on-grid mode of operation, 2.) asset coordination, control of active and reactive power, and keeping the lights on during off-grid mode of operation, and 3.) autosynchronization.

As shown in Fig. 6, the project consists of one 2.112 MVA grid-tied PV inverter controller interfacing with six inverters; two 1.375 MVA BESS inverters managed by a BESS controller, housed with two batteries; and two diesel generators with a total capacity of 1.6 MVA, managed by a generator controller.

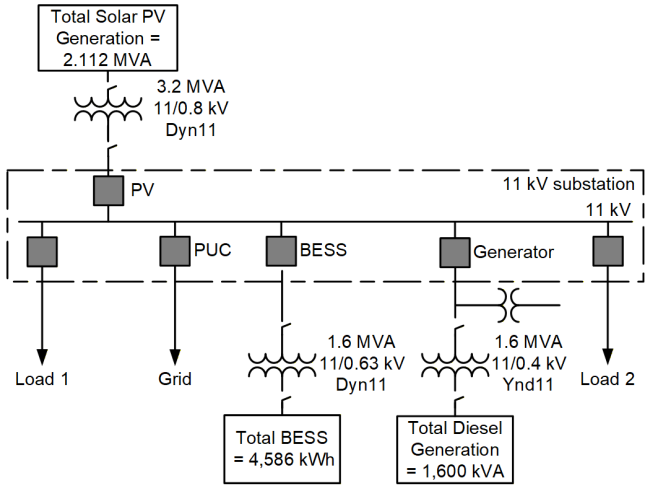


Fig. 6 Simplified single-line diagram.

When the plant is connected to the grid, six PV inverters with a combined capacity of 2.112 MVA and two BESS inverters with a total capacity of 4,586 kWh supply power to the in-house load of the plant. This prioritizes the output from the PV inverters over the BESS inverters, minimizing grid imports. If the plant is islanded, the BESS is the primary power source, functioning as the grid-forming unit, which sets the plant's voltage and frequency references, with the PV inverters following its lead.

V. MCS ARCHITECTURE

Fig. 7 describes the system architecture of the MCS, which comprises four layers [1].

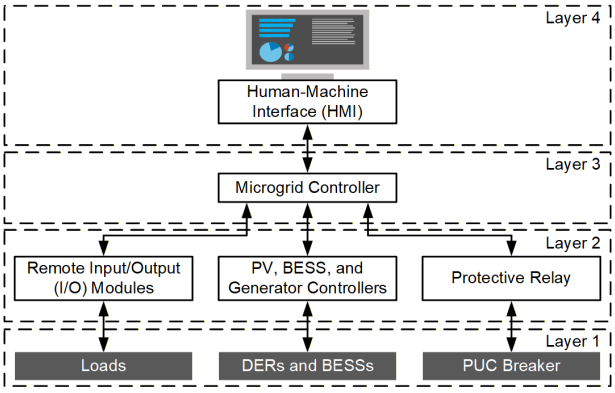


Fig. 7 MCS architecture.

A. Layer 1

Field devices form the system foundation, comprising breakers, BESSs, PV inverters, generator controllers, and remote loads. These devices interface directly with the power

system, providing critical data such as event logs, waveform captures, and real-time measurements, while integrating protection functions to safeguard assets like transformers, motors, and switchgear.

B. Layer 2

Protection and control devices serve as the operational intelligence at the field level, comprising protective relays such as the PUC relay, remote I/O modules, and individual controllers for PV, BESS, and diesel generator sets; these components acquire data from Layer 1 and transmit control commands, ensuring robust and secure system communications, while maintaining autonomous functionality even in the event of higher-layer failures.

C. Layer 3

A microgrid controller represents the centralized control layer, which collects data from Layer 2 and executes real-time decisions to enhance grid performance; it issues commands to field devices for renewable dispatch, energy arbitrage (economic dispatch), peak shaving, power factor (PF) correction, and frequency and voltage control.

D. Layer 4

An HMI constitutes the topmost layer, dedicated to monitoring and engineering, and includes engineering software and diagnostic tools; this layer delivers real-time system status, event analysis, settings management, and economic optimization capabilities, serving operations and maintenance teams with visualization and control functions. Its failure does not compromise the operational integrity of the underlying layers.

VI. Simulation Using Universal Power Flow (UPF) Controller

Traditional power flow simulations use a fixed slack bus and assume constant frequency and voltage, making them suitable for large grids but less effective for microgrids with limited generation, variable frequency, and diverse control strategies [2]. The UPF controller addresses these limitations through flexible generator control modes (isochronous, droop, and constant power), reactive power control options (MVAR, PF, voltage, and voltage droop), and frequency- and voltage-dependent load modeling. During factory acceptance tests (FATs), it enables validation of microgrid functions such as energy arbitrage, peak shaving and autosynchronization under realistic conditions without requiring a slack bus. UPF also models solar irradiance variations using static and dynamic inputs. Dynamic irradiance replicates cloud cover by gradually reducing PV output, allowing evaluation of solar smoothing, where the BESS compensates through discharge. The controller can also simulate BESS SOC for testing critical scenarios. When SOC falls below 20%, the microgrid controller automatically starts a generator to maintain supply continuity. During simulated cloud-cover events, declining PV output was offset by generator support and limited BESS discharge at low SOC, ensuring stable load supply without abrupt transitions. As shown in Fig. 8, the BESS discharged during low-irradiance periods to compensate for reduced PV generation and maintain system stability. Section 7 evaluates the operational and economic benefits of enabling energy arbitrage and peak shaving within the MCS. These functions allow the system to maintain active power set points during peak tariff periods, resulting in significant cost savings, as demonstrated in Section 10. The UPF controller enhances testing by supporting both normal and negative simulation scenarios, including deliberately disabling peak shaving and energy arbitrage. Results from these tests show increased operating costs when these functions are unavailable, highlighting their economic value. This simulation capability enables comprehensive validation of MCS performance for both optimal and adverse conditions while assessing its potential to improve operational efficiency and reduce costs.

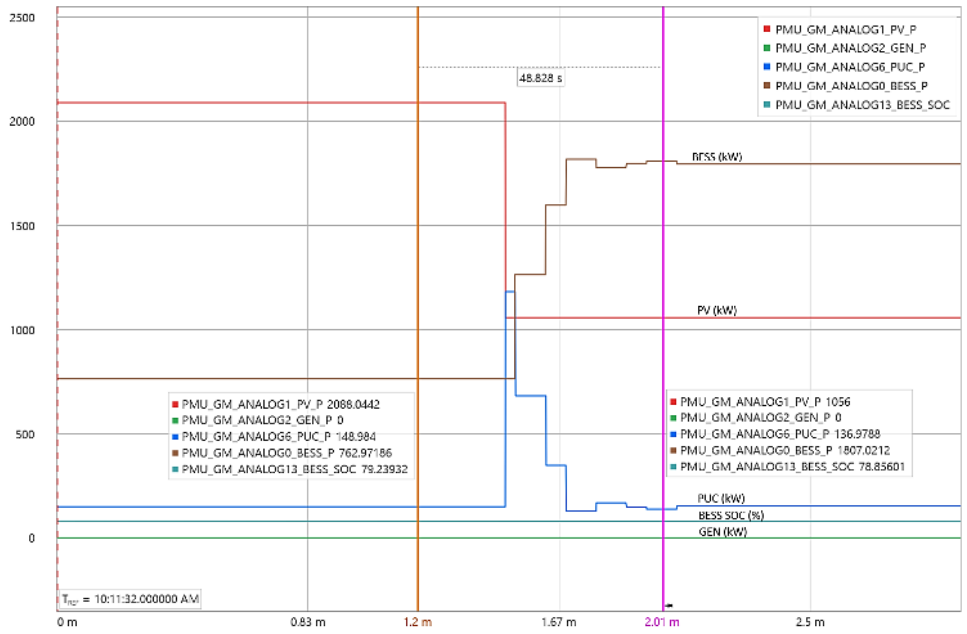


Fig. 8 Solar smoothing with BESS.

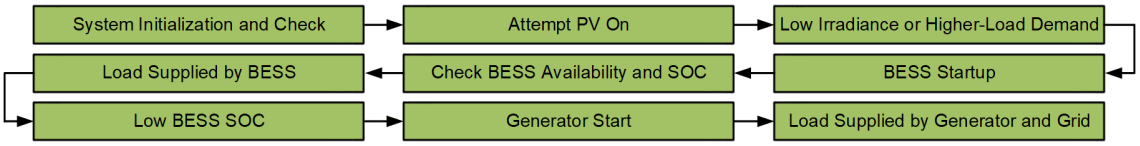


Fig. 9 On-grid mode of operation flowchart.

VII. On-Grid Mode of Operation

The MCS manages the PUC, allowing the facility to interact with the adjacent utility grid. In on-grid mode, the PUC enables the facility to receive power and reliability support from the grid as needed. The flow chart in Fig. 9 shows the control philosophy of the MCS when it is connected to the grid.

The on-grid control algorithm is classified into three sections: 1.) Energy arbitrage (economic dispatch), 2.) Peak shaving, and 3.) reactive power control at the PUC.

Energy arbitrage is implemented to allow operators to strategically manage energy resources based on TOU pricing, optimizing cost savings and system efficiency. The system enables operators to classify any hour within a 24-hour period, from midnight to 11:59 p.m. across all days of the week, in alignment with predefined tariff structures. Operators follow set points that categorize time slots into three distinct levels: Level 1 for peak hours, Level 2 for standard time, and Level 3 for off-peak time. These classifications guide the dispatch strategy, allowing the MCS to prioritize energy storage and generation resources to minimize operational costs and maximize economic performance. The control strategy of the assets is different for each mode.

A. Level 1: Peak Hours

During peak-hour operation (Level 1), the control strategy maintains the PUC active power within the prescribed set point (~150 kW import) through coordinated dispatch of PV generation, BESS, and grid support. Across the evaluated intervals, the BESS predominantly operates in discharge mode to supplement limited PV generation under high-load conditions, thereby constraining grid import to the PUC limit. As PV availability increases, the BESS discharge requirement decreases, transitioning to charging during periods of surplus generation and reduced demand, while still maintaining the PUC constraint. The control system dynamically balances PV output, BESS SOC, and load demand to ensure compliance with the import limit, enabling effective peak shaving, enhanced self-consumption, and economically optimized operation through energy arbitrage. Fig. 10 illustrates a set of 16 test cases performed during an FAT to assess MCS functionality during peak hours.

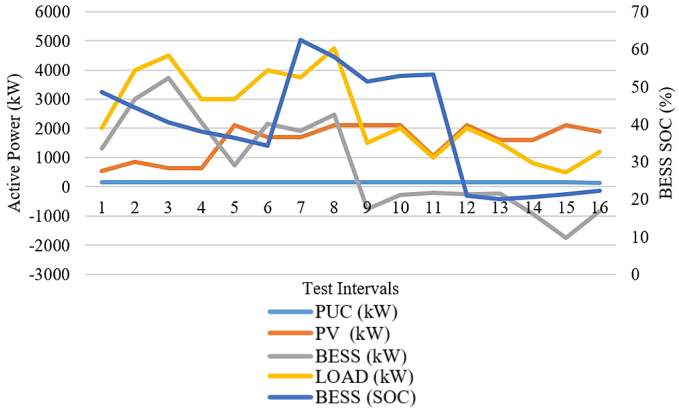


Fig. 10 Energy arbitrage graph showing peak hours (Level 1).

B. Level 2: Standard Hours

During standard-hour operation (Level 2), the control strategy maintains the PUC active power close to the defined set point (~300 kW import) through coordinated dispatch of PV generation, the BESS, and grid interaction. Under varying load and generation conditions, the BESS operates flexibly in both charging and discharging modes to regulate power flow and ensure adherence to the PUC constraint. During periods of PV surplus and lower demand, the BESS predominantly charges, improving energy utilization and supporting arbitrage objectives, while the grid import remains constrained to the set limit. Conversely, during higher-load conditions or reduced PV availability, the BESS provides supplemental discharge to maintain the PUC set point. The results demonstrate effective real-time balancing of PV output, BESS SOC, and load demand, enabling stable operation, controlled grid dependency, and economically optimized performance within the defined standard-hour operating regime. Fig. 11 illustrates 16 test cases executed during an FAT under standard operating hours.

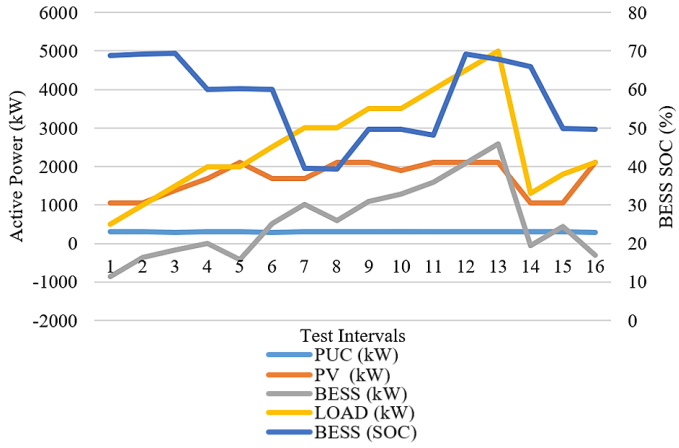


Fig. 11 Energy arbitrage graph showing standard hours (Level 2).

C. Level 3: Off-Peak Hours

During off-peak operation (Level 3), the control strategy maintains the PUC active power close to the specified set point (~750 kW import) through coordinated management of PV generation, the BESS, and grid interaction. Under higher-load and low-to-moderate PV availability, the BESS operates in discharge mode to supplement generation and limit grid dependence while ensuring compliance with the PUC constraint. As load decreases and PV generation increases, the BESS transitions to charging mode, using surplus energy and lower tariff periods to support energy arbitrage objectives. The control system dynamically adjusts BESS power and SOC in response to varying generation and demand profiles, maintaining consistent grid import at the prescribed limit. The results demonstrate effective off-peak operation characterized by enhanced energy absorption, controlled grid interaction, and economically optimized scheduling. Fig. 12 presents 16 representative test scenarios executed during an FAT under off-peak operating conditions.

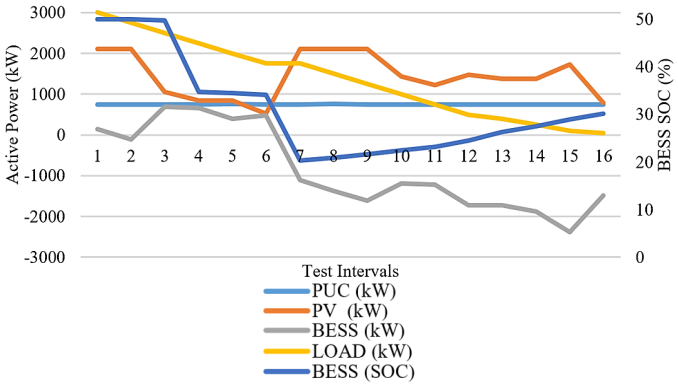


Fig. 12 Energy arbitrage graph showing off-peak hours (Level 3).

D. Peak Shaving

During peak-shaving operation, the control strategy prioritizes maintaining PUC active power within the specified peak-shaving limit (~100 kW), overriding energy arbitrage commands when necessary. As shown in Fig. 13, the BESS operates primarily in discharge mode to reduce peak grid demand, while PV and dispatchable generators supplement the load based on resource availability and SOC. The coordinated control dynamically allocates power among the BESS, PV, and generators, ensuring grid import remains within predefined limits. This approach maximizes onsite resource utilization, minimizes grid dependency during peak pricing periods, and demonstrates effective and reliable peak-demand management.

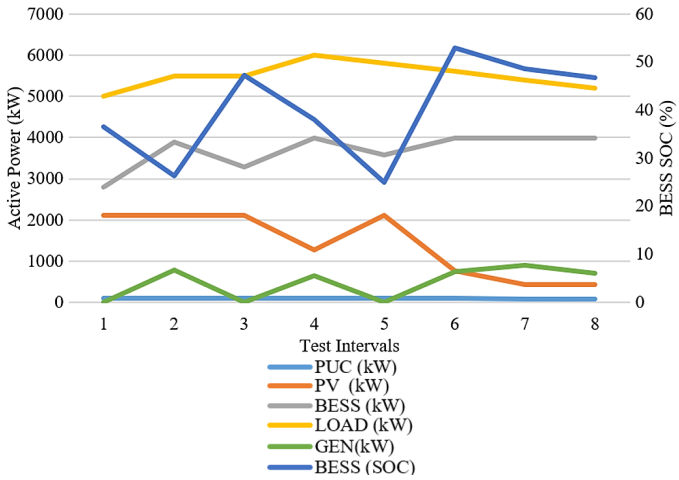


Fig. 13 Peak-shaving graph.

E. Reactive Power Control at PUC

The reactive power control strategy at the PUC regulates reactive power exchange and voltage through coordinated control of DERs, including PV inverters, BESSs, and other VAR-capable assets. By dynamically adjusting the plant reactive power (Q) reference, the controller manages VAR flow at the PUC while ensuring participating inverters operate in VAR control mode. The framework supports three mutually exclusive modes—VAR (Q) control, PF control, and voltage (V) control with only one active at a time. Each mode adjusts the plant-level Q reference to achieve its objective, ensuring stable voltage regulation and compliant reactive power exchange with the utility grid.

1) VAR (Q) Mode

When the Q set point is provided, the controller shall drive the plant to that set point within 30 seconds, as per the South Africa grid code requirements for renewable power plants (Categories B and C) [3].

2) PF Mode

In PF control mode, the controller regulates the plant PF by continuously computing and dispatching the required reactive power set point based on real-time operating conditions and active power output. With PF mode enabled, the controller calculates the dynamic Q set point based on Equation (1).

$$Q_{set} = P \bullet \sqrt{\frac{1}{PF^2 - 1}} \quad (1)$$

where:

P is the active power at the PUC.

PF is the desired power factor the microgrid controller is expected to drive the plant to.

3) Voltage (V) Mode

In voltage control mode, the system maintains the desired voltage at the PUC by dynamically modulating the reactive power injection or absorption. With V mode enabled, the controller calculates the dynamic Q set point based on Equation (2).

$$Q_{set} = \frac{(V_{set} - V_{plant}) \cdot 2 \cdot Q_{max}}{V_{rated} \cdot droop} \quad (2)$$

where:

Q_{max} is the maximum reactive power capacity of the power plant.

V_{rated} is the rated voltage at the PUC.

Droop is the curve that defines the amount of Q to change for the desired voltage at the PUC.

VIII. Off-Grid Mode of Operation

During off-grid operation, where the PUC is unavailable, the MCS prioritizes process survivability, commonly referred to as keeping the lights on. In this mode, the BESS assumes the role of the grid-forming asset, initiating VSG mode for the PV inverters to maintain system stability and frequency and voltage references. The MCS continuously monitors system parameters, such as frequency and SOC. These strategies involve prioritizing and disconnecting nonessential loads to preserve critical operations. Upon restoration of grid availability, the BESS facilitates a manual autosynchronization process, referred to as live bus synchronization, ensuring a seamless transition back to grid-connected mode without disrupting ongoing operations. Section 9 discusses the technical details and implementation of this synchronization process. This layered approach to control and resilience underscores the capability of the MCS to maintain operational continuity and optimize energy management under varying grid conditions. Fig. 14 shows the control philosophy of the MCS when it is disconnected from the grid.

IX. Autosynchronization

The MCS achieves seamless synchronization through a delta-change control algorithm that continuously monitors voltage, frequency, and phase-angle differences between a DER, such as a BESS, and the grid or microgrid bus. The algorithm calculates parameter rates of change and applies real-time corrective actions to reduce deviations, ensuring smooth convergence to synchronization conditions. For BESS applications, it regulates the ΔV between the PUC and inverter bus using coordinated voltage and phase control, typically supported by a phase-locked loop. Once voltage, frequency, and phase-angle deviations fall within predefined limits, the controller initiates automatic breaker closure. This adaptive approach minimizes transients, improves system stability, and enables reliable autosynchronization, load sharing, and microgrid reconnection.

The utility's standard interconnection limits are: 1.) maximum frequency difference (Δf) ≤ 0.1 Hz, 2.) maximum voltage difference (ΔV) ≤ 3%, and 3.) maximum phase angle difference ($\Delta\phi$) ≤ 10°, in accordance with typical synchronizing parameter limits (IEEE 1547, p. 12) [4]. These thresholds are especially relevant for BESSs because of their rapid response and precise voltage and frequency control. BESS inverters can adjust output in real time to align with grid conditions, making them effective for synchronization support during renewable energy fluctuations or load imbalances. Their integration also improves grid resilience and supports black start, frequency regulation, and voltage support during reconnection. Compliance with synchronization requirements is essential for maintaining grid stability and protecting infrastructure.

The autosynchronization relay provides the microgrid controller with line and bus frequency, voltage, and phase angle measurements, along with their respective differences. The controller sends frequency and voltage adjustments to the BESS until all differences fall within the deadband, after which the PUC relay issues a breaker close command. To reconnect to the grid, the BESS synchronizes to the restored municipal supply. If closure conditions are satisfied, the PUC breaker is closed and the microgrid controller returns the inverters to active and reactive power (PQ) mode.

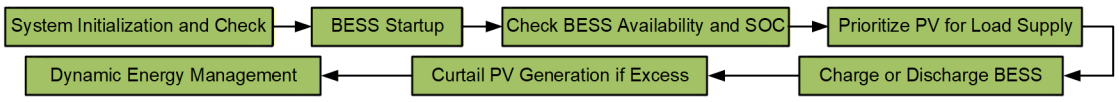


Fig. 14 Off-grid mode of operation flowchart.

X. CONCLUSION

Fig. 15 demonstrates the result of enabling peak shaving and energy arbitrage features with the MCS.

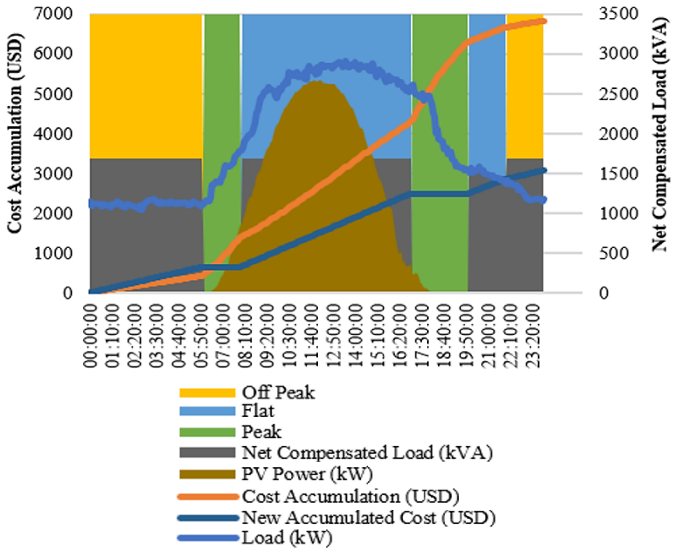


Fig. 15 Result of peak shaving and arbitrage with PV supplying energy deficit.

By examining the two cost accumulation trends, a notable reduction in both daily and monthly electricity costs can be observed, as summarized in Table IV. This comparison demonstrates the financial impact of demand optimization measures, confirming that strategic load management and peak reduction directly contribute to lower overall energy expenditure over time. The reductions from Table IV reflect energy cost savings and exclude the impact of maximum demand savings. Incorporating the maximum demand savings quantified by the difference between Table II and Table III adds ZAR 360,588.50 (approximately USD 20,569.80) per month to the total benefit.

TABLE IV TOU SAVINGS DURING HIGH-DEMAND SEASON

Currency	Per Day	Per Month
ZAR	52,346.22	1,046,924.4
USD	2,986.10	59,721.87

Fig. 16 illustrates the degree of alignment between the ideal load-shifting solution presented in Fig. 6 and the actual system performance as dispatched by the MCS. The close correspondence between the two profiles demonstrates the effectiveness of the MCS dispatch strategy in approximating the theoretical optimal load behavior under real operating conditions.

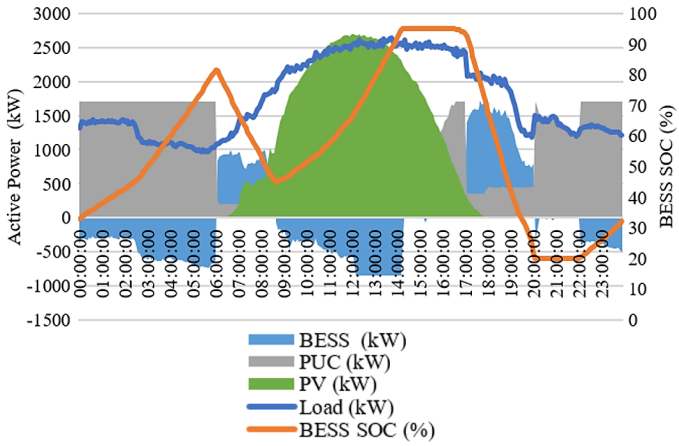


Fig. 16 Example use case for comparison.

This paper demonstrates the successful implementation of an MCS tailored to the South African energy landscape, integrating PV, a BESS, and a diesel generator to optimize energy dispatch, peak shaving, and energy arbitrage. Through advanced synchronization, adaptive load management, and simulation-based validation, the system improves operational resilience, maintains continuity during grid outages, and reduces both energy and maximum-demand costs. Results highlight the value of coordinated DER dispatch under frequent load-shedding conditions. Key lessons learned include the importance of simulation-based validation, SOC-aware dispatch strategies, and grid-forming BESS operation to enable stable transitions between grid-connected and islanded modes. By addressing DER coordination challenges and validating performance across diverse operating scenarios, the proposed framework provides a scalable and robust solution for modern microgrids.

Future work will focus on extending the framework to larger, multisite microgrids, integrating advanced load and renewable generation forecasting, and enabling coordinated control of distributed assets to further improve system reliability, scalability, and economic performance under dynamic grid conditions.

XI. BIBLIOGRAPHY

[1] S. Manson, K. G. Ravikumar, and S. K. Raghupathula, “Microgrid Systems: Design, Control Functions, Modeling, and Field Experience.” (*Wide-Area Protection and Control Systems: A Collection of Technical Papers Representing Modern Solutions*, 2017).

[2] N. Cai and A. R. Khatib, “A Universal Power Flow Algorithm for Industrial Systems and Microgrids—Active Power.” (IEEE Transactions on Power Systems, Vol. 34, No. 6, November 2019, pages 4900-4909).

[3] Grid Connection Code for Renewable Power Plants (RPPs) Connected to the Electricity Transmission System (TS) or the Distribution System (DS) in South Africa–Version 3.1. (National Energy Regulator of South Africa (NERSA), January 2022).

[4] 240-61268576, Eskom: Standard for the Interconnection of Embedded Generation – Revision 1. (October 2018).

© 2026 by CIGRE.
Previously presented at the 22nd Annual GCC CIGRE International Conference, Muscat, Oman
20260715 • TP7282-01